Excitation-Emission Fluorescence Spectroscopic Analysis in the Presence of Interferents: A Laboratory Experiment Integrating Analytical Chemistry and Advanced Data Processing

Valeria Boeris, Miguel A. Cabezón and Alejandro C. Olivieri*

Departamento de Química Analítica, Facultad de Ciencias Bioquímicas y Farmacéuticas, Universidad Nacional de Rosario e Instituto de Química Rosario (IQUIR-CONICET), Suipacha 531, Rosario (2000), Argentina, aolivier@fbioyf.unr.edu.ar

Received January 5, 2013. Accepted May 18, 2013.

Abstract: In the present report an advanced experiment is described to introduce chemistry students to the direct chemometric resolution of binary mixtures of two pharmaceuticals (oxatomide and phenylephrine) by measuring excitation-emission fluorescence matrices, and processing them with second-order calibration based on a decomposition algorithm called parallel factor analysis (PARAFAC). This experiment is of interest because it combines experimental analytical chemistry (preparation of standard solutions, spectrofluorimetric measurements, etc.) with computer applications not requiring deep programming skills. Second-order multivariate calibration was implemented with a simple graphical toolbox especially designed for this report: mvc2basic, which is available as supplementary material. This work provides students the opportunity to be introduced to advanced chemometrics activities in an accessible manner.

Introduction

Spectrofluorimetry is a rapid, accurate and sensitive method for the determination and quantification of fluorescent or fluorescent-derivative compounds [1–6]. However, the use of spectrofluorimetry for determining an analyte in a mixture may become difficult if additional fluorescent components occur [7]. In these cases, suitable analytical strategies involve: (1) physical separation of the analyte from other sample components, e.g., chromatography, (2) sample pre-treatment or clean-up for interferent removal prior to analyte determination, or (3) mathematical separation of component signals using chemometrics.

Chemometrics is a subdivision of chemistry that uses computational methods for qualitative and/or quantitative analysis of measurement data. In the framework of analytical chemistry, chemometric computational methods have been designed for calibration and evaluation of unknowns in samples of different degrees of complexity [8]. Of particular interest to the present report are multivariate calibration methods, i.e., those based on the measurement of multiple data for each experimental sample, and aimed at analytical calibration purposes.

In the last decades, these methods have been introduced for the analysis of increasingly complex samples, accompanying the progress in chemical instrumentation, which is delivering data with a structure of growing complexity. First-order data, e.g., spectra, are ubiquitous in this regard, as reflected by the popularity of chemometrics-assisted near infrared spectral analysis, which is widespread in many industrial applications [9–12].

When data for a single chemical sample comprise a data matrix, we enter the second-order domain. These data can be suitably organized into a table with two different and independent measurement modes, which can be conveniently visualized as a two-dimensional surface or landscape as shown in Figure 1.

The main advantage of employing second-order over first-order data for analytical calibration is the possibility of a direct separation of the measured signals into the underlying contributions from individual analytes [8]. This is due to the fact that second-order data lead to data arrays which can be uniquely decomposed, allowing relative concentrations and profiles of the individual components in the different domains to be extracted directly. In this way, analytes can be quantified even in the presence of unknown interferents which are not included in the calibration set, a property known as the "second-order advantage" [13,14].

Excitation-emission fluorescence matrices (EEMs) are second-order data which present certain advantages: (1) measurements may be conveniently carried out on a single instrument, (2) fluorescence signals are sensitive and selective, and (3) the obtained data have a simple mathematical structure, which can be analyzed using an intuitively appealing model called parallel factor analysis (PARAFAC) [15–17].

The combination of spectrofluorimetric data and chemometric tools such as PARAFAC has allowed simplification of experimental procedures and direct determination of many analytes including therapeutic drugs [14, 16, 18, 19]. Some preliminary sample preparation steps can be eliminated, replacing the physical separation of interferences by the chemometric separation of their signals [7, 8, 20, 21].

In the present report we wish to introduce chemistry students to the direct chemometric resolution of binary mixtures of two pharmaceuticals by performing EEM fluorescence measurements and applying second-order calibration based on PARAFAC. This experiment is of interest because it combines experimental analytical chemistry (preparation of standard solutions, spectrofluorimetric measurements, etc.) with computer applications (second-order

 S1430-4171(13)0xxxx-x, Published xx/xx/2013, 10.1333/s00897132491a, xxxxxxaa.pdf

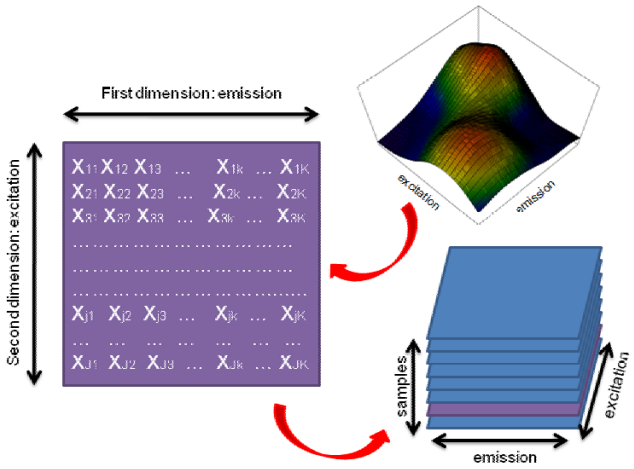

Figure 1. Organization of a data matrix into a table and its visualization as a three-dimensional surface. Bottom-right: a three-way data array built from the collection of data matrices for several samples of varying composition.

multivariate calibration implemented with a simple toolbox not requiring significant programming skills). Figures of merit, such as sensitivity, selectivity and limit of detection can also be estimated for the proposed method using the same software [22, 23].

The studied pharmaceuticals are oxatomide {OXA, 1-[3-(4-benzhydrylpiperazin-1-yl)propyl]-benzimidazolin-2-one}, a histamine H1-receptor antagonist piperazine derivative used for the symptomatic relief of hypersensitivity reactions including urticaria, rhinitis, and conjunctivitis [24], and phenylephrine [PHE, (R)-2-methylamino-1-(3-hydroxyphenyl) ethanol], a sympathomimetic agent with direct effects on alpha-adrenoreceptors, mainly employed as a nasal decongestant [25]. The corresponding chemical structures are shown in Figure 2. These compounds are both non-toxic and commercially available, which make them appropriate to be used in a teaching laboratory.

Theory

Spectrofluorimetric data. The fluorescence emission intensity of a solution of a single pure fluorescent constituent is proportional to its concentration, to its molar absorption coefficient at the excitation wavelength and to its relative emission coefficient at the emission wavelength [26]. For reasons of consistency with the nomenclature usually employed in chemometric data processing of fluorescence data, these parameters are here represented, respectively, by x (intensity), a (concentration), b (extinction coefficient) and c (emission coefficient), i.e.:

$$x = a\,b\,c \qquad (1)$$

Additionally, the fluorescence of a solution containing more than one fluorescent constituent is equal to the arithmetic sum of fluorescent signals of each constituent. i.e. [27]:

$$x = (a\,b\,c)_1 + (a\,b\,c)_2 + \ldots + (a\,b\,c)_N = \sum_{n=1}^{N} (a\,b\,c)_n \qquad (2)$$

where n represents the index for each constituent and N the total number of constituents.

Parallel factor analysis (PARAFAC). PARAFAC is a mathematical model suitable for analyzing spectrofluorimetric data based on equation (2). The latter expression corresponds to the fluorescence signal of a given sample measured at given excitation and emission wavelengths. If measurements are made within a certain spectral range at multiple wavelengths, the fluorescence values can be arranged into a data table with two entries: the excitation wavelength (with index j ranging from 1 to J) and the emission wavelength (with index k ranging from 1 to K). A generic element of this excitation-emission matrix $\mathbf{X}$ is thus x_{jk}. When measurements for several samples of varying compositions are made, these data matrices can be placed on top of each other to build a mathematical object with three modes or ways, i.e., a three-way data array $\boldsymbol{X}$, as shown in Figure 1. If i is the sample index running from 1 to the total number of samples I, a generic element of the three-way data array is given by:

$$x_{ijk} = \sum_{n=1}^{N} a_{in}\, b_{jn}\, c_{kn} \qquad (3)$$

which derives from equation (2) when multiple samples are considered. The above model is known as *trilinear*, because the signal is linear in a (for fixed b and c), linear in b (for fixed a and c) and linear in c (for fixed a and b).

Decomposing the three-way array $\boldsymbol{X}$ consists in estimating the values of a_{in}, b_{jn} and c_{kn} for all the N components of the mixtures. Usually this is done by least-squares fitting, i.e., minimizing the sum of the squared error models $(e_{ijk})^2$ in the expression:

$$x_{ijk} = \sum_{n=1}^{N} a_{in}\, b_{jn}\, c_{kn} + e_{ijk} \qquad (4)$$

PARAFAC has physical connotation and often provides unique solutions, which is a great advantage for modeling spectroscopic data, because true underlying spectra will be found [28]. The usual output of the software implementing PARAFAC consists of three matrices, as shown Figure 3: (1) a so-called score matrix $\mathbf{A}$, of size $I \times N$, containing the values of the a_{in} elements, which are the relative concentrations of all components in all samples, (2) a loading matrix $\mathbf{B}$ of size $J \times N$, containing the generalized profiles representing the excitation spectra of the N components at the J excitation wavelengths, and (3) a second loading matrix $\mathbf{C}$ of size $K \times N$, containing the generalized profiles representing the corresponding emission spectra [17]. The profiles in both data modes are usually normalized to unit length, i.e., for each component profile the sum of the squared elements is 1. The relative concentrations contained in matrix $\mathbf{A}$, on the other hand, have an arbitrary scale, and do not provide the component concentrations directly. A calibration procedure is required to accomplish analyte determination, as described below.

Calibration with PARAFAC. After the decomposition step, analyte determination proceeds by following this protocol. First the analyte index should be identified in the matrix $\mathbf{A}$, because the PARAFAC software provides the scores in the order of their contribution to the total signal. This

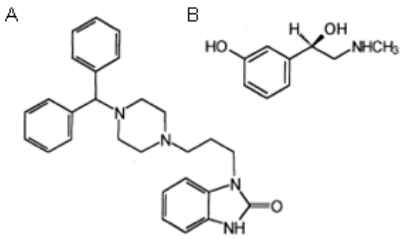

Figure 2. Chemical structures. A) OXA. B) PHE.

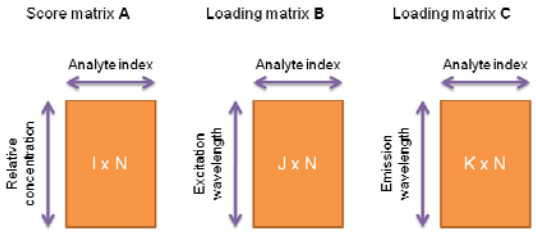

Figure 3. Block representation of the PARAFAC output matrices **A**, **B** and **C**.

identification is done by comparing the corresponding profiles contained in matrices **B** and **C** with spectra for pure standards to the analyte of interest. Once the analyte index *n* is known, the *n*th. column of matrix **A** is extracted. It contains as many scores as samples have been employed to build the three-way array decomposed by PARAFAC. One of them corresponds to the unknown sample, and the remaining ones to the calibration samples. The latter ones are employed to build a pseudo-univariate calibration graph, from which the slope and intercept are estimated by least-squares linear regression. Finally, the score for the analyte in the unknown sample is interpolated in the latter plot, and the analyte concentration is estimated. Further details are provided below concerning the specific experiment described in the present report.

Experimental

The experimental and data processing sections of this work are proposed to be carried out in three 3-hours sessions. However, a previous session can be added if the teacher is interested in introducing students to searching bibliography; if this option is feasible, the spectral range of data collection will be decided in discussions with the students based on previous literature reports, instead of directly providing them with the emission and excitation wavelength ranges to be employed in the experiment. In addition, the students can also determine by themselves the concentration range of the calibration samples and the parameters used in the fluorescence measurement, such as the voltage of the detector and the excitation and emission slit widths. These experimental activities will not be discussed here, as they are standard operational procedures of any spectrofluorimetric determination [3, 29]. The estimated time required for each activity is shown in Table 1.

Reagents. OXA (Janssen-Cilag Laboratories, Buenos Aires, Argentina) and PHE (POEN SACIFI Laboratories, Buenos Aires, Argentina) were of analytical grade quality. Stock solutions of OXA (50 mg L^{-1}) and PHE (20 mg L^{-1}) were prepared by accurate weighing of the reagents and dissolution in aqueous 50 mM HCl. Accurate volumes of each stock solution were transferred into 5.00 mL volumetric flasks and diluted to volume with 50 mM HCl to prepare the working solutions (calibration and test).

Two sets of 6 samples each were prepared for calibration of each analyte, as shown in Table 2. The concentrations of the calibration solutions were equally spaced from 0.00 to 0.50 mg L^{-1} and from 0.00 to 2.00 mg L^{-1} for OXA and PHE, respectively. These concentration ranges were determined taking into account that the fluorescence intensity of PHE is weaker than that for OXA. By using more concentrated PHE solutions, the fluorescence signals for both analytes become comparable.

Five test samples (A-E) were prepared with random concentrations of both analytes, and a sixth one (F) with analyte concentrations which were half the maximum concentrations of the calibration solutions, as shown in Table 3.

The whole idea of the presently described experiment is to show students that one can produce a calibration model based on pure analyte solutions of OXA (contained in one of the two 6-sample calibration sets), and predict the OXA concentration in test samples containing mixtures of OXA and PHE, even when the signals for both constituents overlap. Likewise, it can be shown that using the remaining 6-sample calibration set built with pure PHE solutions, one may predict the content of PHE in the test sample mixtures. This is one of the great advantages of calibration with second-order data, as explained above when introducing the expression "second-order advantage".

Apparatus and software. Fluorescence excitation-emission matrices were collected on a Perkin Elmer LS 55 spectrofluorimeter equipped with a pulsed xenon lamp, and using 1.00 cm polymethacrylate cells. Once measured, the matrices were saved in ASCII-compatible form using the equipment software.

The data were then handled using the MATLAB computer environment [30]. The calculations involved in the mixture resolution by PARAFAC have been made using mvc2basic, a MATLAB graphical interface toolbox. This toolbox accepts a variety of input data formats contained in ASCII files (matrices or vectors), allows for the manual selection of working wavelength regions, and plots landscapes for selected samples. The development of each model and its subsequent application to unknown samples is straightforward. The toolbox, operating manual and example data have been deposited as Supplementary Material accompanying the present report. It is a simplified version of the complete MVC2 toolbox [23], and can be freely downloaded, including a detailed manual and example data from the web page www.iquir-conicet.gov.ar/descargas/mvc2basic.rar.

Protocol. *Selection of the excitation and emission wavelength ranges.* Taking into account previous literature reports [24, 31, 32], the spectral range selected to measure the native fluorescence of OXA and PHE were from 240 to 288 nm for excitation and from 290 to 360.5 nm for emission. Figure 4 illustrates that binary mixtures of OXA and PHE cannot be determined by conventional fluorescence, since they show strongly overlapping spectra.

Obtaining the excitation-emission matrices. According to the characteristics of the spectrofluorimeter, the emission wavelength was, by default, incremented by 0.5 nm in the selected range. On the other hand, the excitation wavelength was selected to be incremented by 2 nm to obtain a reasonable amount of data, allowing an appropriate resolution without increasing the processing time. The detector voltage was fixed at 900 V and the slit widths at 5 nm. The scanning rate was 1000 nm/min.

Data files preparation. Once the EEMs for the calibrations and test samples were recorded and saved, a previous step is required before the calculation by the mvc2basic toolbox [23]. In the same folder in which the EEM text files were saved, some new files needed for the data processing were also created:

- Y_OXA.TXT and Y_PHE.TXT: these are single-column files containing the calibration concentrations of each analyte in each of the two 6-sample calibration sets.
- CALFILESOXA.TXT and CALFILESPHE.TXT: these are single-column files containing the filenames of the calibration data matrices, in the same order as the concentrations appear in the Y_OXA.TXT and Y_PHE.TXT files.

Table 1. Estimated time required for each activity

Class	Activity	Estimated required time (min)
1	Introduction	60
	Literature search	60
	Protocol design	60
2	Familiarization with the spectrofluorimeter, preparation of solutions, dilutions, etc. (if needed).	90
	Determination of the parameters for the fluorescence measurements	
	Preparation of the stock solutions	30
	Preparation of the calibration samples	60
3	Preparation of the test samples	60
	Obtaining the excitation-emission fluorescence matrices	120
4	Data files preparation	60
	Calculation and discussion of the results	120

Table 2. Composition of the calibration samples

[OXA] (mg L^{-1})	Stock volume (μL)	Filename	[PHE] (mg L^{-1})	Stock volume (μL)	Filename
0.00	0.0	OXA00.txt	0.00	0.0	PHE00.txt
0.10	10.0	OXA01.txt	0.40	100.0	PHE04.txt
0.20	20.0	OXA02.txt	0.80	200.0	PHE08.txt
0.30	30.0	OXA03.txt	1.20	300.0	PHE12.txt
0.40	40.0	OXA04.txt	1.60	400.0	PHE16.txt
0.50	50.0	OXA05.txt	2.00	500.0	PHE20.txt

Table 3. Composition of the test binary samples

Sample	[OXA] (mg L^{-1})	[PHE] (mg L^{-1})	OXA stock volume (μL)	PHE stock volume (μL)	Filename
A	0.427	0.178	42.7	44.5	mixA.txt
B	0.453	0.556	45.3	139.0	mixB.txt
C	0.064	1.594	6.4	398.5	mixC.txt
D	0.456	1.916	45.6	479.0	mixD.txt
E	0.316	1.930	31.6	482.5	mixE.txt
F	0.250	1.000	25.0	250.0	mixF.txt

Calculations. The program mvc2basic is run from the directory where the above data are located. It involves a single main window, as shown in Figure 5A, from which all steps required to implement the second-order multivariate calibration strategy can be carried out. In the present case, the empty fields of this window should be filled as follows:

- The field labeled "Number of components" is filled according to the number of components in the sample. In this work this number was determined as explained in the Results section.
- The "Sensor data" field requires the indexes of the data matrices: 290 is the first sensor in mode 1 (emission), 360.5 is the last sensor in mode 1, 0.5 is the separation between sensors in mode 1 (there are 142 data points in mode 1), 240 is the first sensor in mode 2 (excitation), 288 is the last sensor in mode 2 and 2 is the separation between sensors in mode 2 (there are 25 data points in mode 2).
- To select wavelength ranges, the "Selected data" space was filled with appropriate values in order to restrict the ranges, mainly to avoid unwanted phenomena such as scattering. These values were determined as explained in the Results section.
- "X_matrices" was selected from the drop down list in the "Data type" field. Here it is important to point out that it is necessary to know in advance the type of file that the instrument creates when the EEM data are saved.
- To analyze each test sample, the field "Single unknown X" was filled with the filename of the file containing the EEM data (MIXA.TXT, MIXB.TXT, …), and the field "Calibration X files" was filled with the corresponding filename (CALFILESOXA.TXT or CALFILESPHE.TXT), depending on the analyte to be quantified.
- By default, the "Method" is fixed at PARAFAC, and "Sample type" at "single unknown". More options are available in the advanced toolbox MVC2 [23].
- In order to visualizate a given data matrix as a surface plot, the name of the file containing the matrix of interest can be writen in the "Plot sample" field, clicking then in the "Plot" buttom. The plot appears in a separate window, as shown in Figure 5B.
- The information which has been entered on a particular screen can be saved by pressing "Save screen". In this way, the next time mvc2basic is run, the screen will automatically appear with the saved information.

After all fields have been completed, the analysis is started by pressing the "PREDICT" button.

Results

Issues relevant to the application of the PARAFAC model to three-way fluorescent data are: (1) how to establish the number of components, (2) how to identify specific fluorescent components from the information provided by the model, and (3) how to calibrate the model in order to obtain absolute concentrations for a particular component in an unknown sample.

Estimating the number of components and selecting the wavelength range. All implemented methods require a certain number of responsive components to be preset for building the calibration model. In the case of trilinear decomposition models such as PARAFAC, the number can be set by analyzing the residuals of the least-squares fit of the three-way data array to the trilinear model. This parameter stabilizes when the correct number of components has been reached [16].

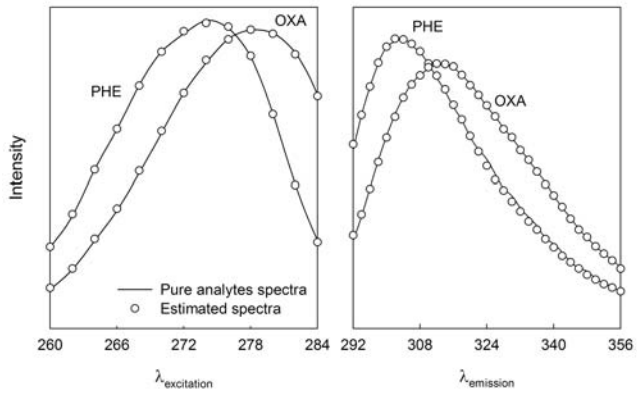

Figure 4. Emission and excitation spectra of OXA and PHE. Solid lines: experimental spectra recorded for pure analytes. Dots: PARAFAC estimated spectra obtained by analysis with mvc2basic.

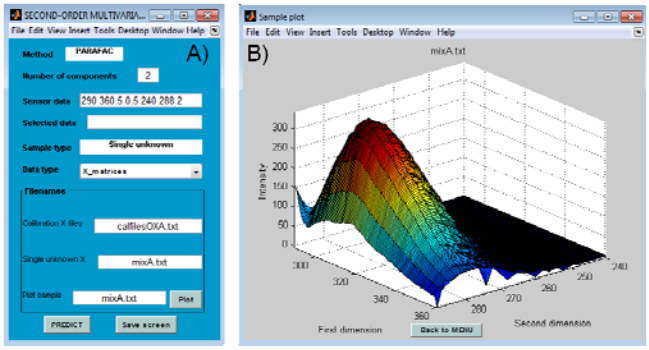

Figure 5. A) Main mvc2basic screen. Each field was filled in order to determine OXA in sample A, considering 2 components and using full wavelength ranges. B) Landscape visualization of data for sample A using the "Plot" option of mvc2basic.

Table 4 shows the standard deviation of the fitting residuals as a function of a trial number of components, when the sample F was processed together with each calibration sample set. As can be seen, the analysis of the residual fit leads to the conclusion that three responsive components are present in these samples, because the standard deviations of the fitting residuals stabilize for three components. However, this number is not in agreement with the known number of components (analytes + interferent species), which should be required by the PARAFAC algorithm. As the components in the samples are only two (OXA and PHE), we analyzed both the excitation and emission profiles obtained by setting the number of components to three, to understand what was the origin of the discrepancy. As Figure 6A shows, the first and second components correspond to OXA and to PHE respectively, but the third one seems to represent a scattering effect. In the latter profiles, the major peak represents the Rayleigh dispersion, since the maxima correspond to equal excitation and emission wavelengths, while the minor peak is probably a Raman dispersion from the solvent. This provides the opportunity of discussing with students dispersion effects appearing in fluorescence spectroscopy, which should be distinguished from true fluorescence phenomena.

To avoid the presence of dispersion signals that are uncorrelated with the target concentrations of the studied analytes, and which do not obey the trilinear model, it would in principle be necessary to record new EEM data (one for each sample, including test and calibration sets) in appropriate wavelength ranges. However, the toolbox mvc2basic allows one to avoid this extra work, since it permits the selection of restricted wavelength ranges from the original EEMs, according to the above mentioned considerations. Therefore, the EEMs were in all cases processed in the sensible excitation and emission ranges where only the analytes contribute to the overall fluorescence intensity, that is, emission range from 292 to 356 nm, and excitation range from 260 to 284 nm, as shown in Figure 6B. When the wavelength ranges were modified in this manner, the standard deviations of the fitting residuals were determined again trying different number of components. As shown in Table 4, they stabilize at two components under these processing conditions. Subsequently, data processing was carried out considering two PARAFAC components in the restricted wavelength ranges.

Identifying the components. The test samples were studied by determining each of the analytes at a time, using the corresponding calibration solutions, and considering the remaining constituent as an interference. Identification of the chemical constituents under investigation was done by comparing the estimated profiles (Figure 6B) with those for the standard solutions of the analyte of interest (Figure 4). This is required since the components obtained by decomposition of the signal are sorted according to their contribution to the overall signal.

After introducing the profile index matching the calibrated analyte, and the filename with calibration concentrations for the same analyte, the button "Go" was clicked to get, in a separate window, the pseudo-univariate calibration graph, as shown in Figure 7. When the profile of each analyte is correctly recognized, the pseudo-univariate calibration plot looks like the one shown in Figure 7A. In this graph, the blue circles represent the calibration samples and the red cross the test sample. If the analyte is misidentified, the pseudo-univariate calibration plot would appear as in Figure 7B. The mistake should be corrected by changing the information provided in the "PARAFAC profiles" window (Figure 6B).

Figure 4 shows the estimated and the pure spectra of OXA and PHE. It is remarkable that the model precisely estimates the two pure spectra, even though the excitation and emission spectra of OXA and PHE are very similar.

Determining the absolute concentrations of each analyte. Absolute analyte concentrations are obtained after calibration, because the three-way data array decomposition only provides relative concentration values. Calibration is performed by means of the set of standards with known analyte concentrations. It involves first decomposing the three-way data array formed by joining the EEMs for the calibration samples with that for the unknown. This method takes advantage of the unique decomposition of the three-way data array, thus allowing obtaining the concentration of the analyte of interest in the presence of any number of uncalibrated interferents. It should be noticed that employment of this mode implies that the three-way data array decomposition should be repeated for each newly analyzed sample.

To obtain the estimated concentration of the analyte, the button "Go" of the window "Calibration line" (Figure 7A) is clicked and the MATLAB space shows:

PARAFAC Results:
Concentration for component 1: 1.04
To calculate AFOMs press the 'AFOM' button

Table 4. Standard deviation of fitting residuals as a function of trial number of PARAFAC components[a]

Number of components	Full wavelength range		Restricted wavelength range	
	OXA	PHE	OXA	PHE
1	7.7	11	9.4	13
2	3.8	5	2.8	2.8
3	2.2	2.2	2.5	2.7
4	2.1	2.2	2.4	2.3
5	2	2.1	2.3	2.3
6	2	2.1	2.2	2.3

[a] Optimum values in boldface.

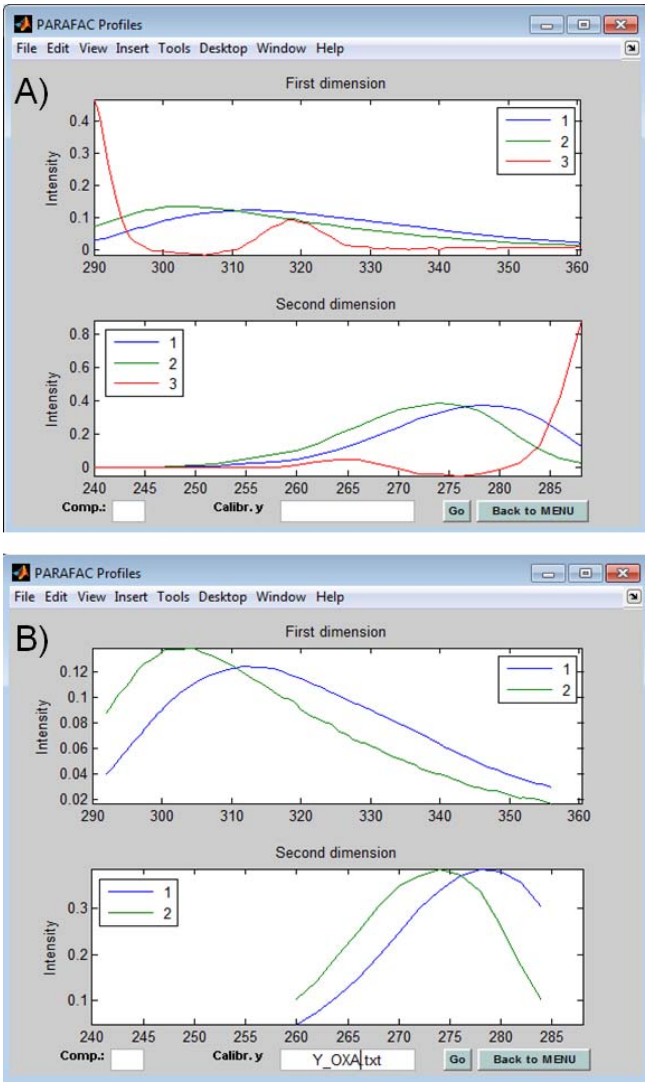

Figure 6. Emission and excitation profiles calculated by PARAFAC using mvc2basic considering: A) Three components in the full wavelength ranges. B) Two components in the restricted wavelength ranges.

In order to calculate the analytical figures of merit, the "AFOM" button in the pseudo-univariate calibration graph is pressed. Sensitivity, analytical sensitivity, selectivity, etc. are provided in the MATLAB space after entering the indexes corresponding to the so-called interferents, i.e., the components not included in the calibration set.

Table 5 shows the concentrations estimated of both analytes in the six binary test samples. In general, PARAFAC yields satisfactory results for the presently studied samples, i.e., the trilinear model applied to EEM fluorescence signals has proved to be useful to accurately predict analyte concentrations in the binary test samples, even in the presence of uncalibrated analytes. Despite the highly overlapped spectra, it was possible to determine each analyte in the presence of the other one, even when the latter was not present in the calibration set. This should convince students that three-way arrays (obtained from second-order data) can be uniquely decomposed by PARAFAC, allowing relative concentrations and profiles of the individual components in the different domains to be extracted directly, recognizing, in this way, the second-order advantage.

For the evaluation of the predictive ability of this multivariate calibration model, the root mean square error of prediction (RMSEP) and relative error of prediction (REP) can be used:

$$\mathrm{RMSEP} = \sqrt{\frac{\sum_{t=1}^{T}(y_{\mathrm{pred},t} - y_{\mathrm{nom},t})^2}{T}} \qquad (5)$$

$$\mathrm{REP} = 100\frac{\mathrm{RMSEP}}{\bar{y}_{\mathrm{cal}}} \qquad (6)$$

where $y_{\mathrm{pred},t}$ is the predicted concentration in each sample, $y_{\mathrm{nom},t}$ the nominal value of the concentration in the sample, T the number of test samples, and $\bar{y}_{\mathrm{cal}}$ the mean calibration concentration. The RMSEP and REP values are also shown in Table 5, confirming than the prediction results are very good.

Table 5 also shows the figures of merit obtained by the analysis for each analyte. These values help the analyst to better appreciate the limitations and advantages of the proposed method. Sensitivity is defined as a function of the slope of the pseudo-univariate calibration curve and the spectral overlapping in both data modes, and can be considered as the change in the net response of the instrument when the concentration of the analyte of interest is increased in one unit. Selectivity measures the degree of overlap of the compound of interest with the remaining sample constituents. Analytical sensitivity is defined as the ratio between sensitivity and instrumental noise, and its reciprocal value defines the minimum concentration difference that can be appreciated across the linear range of the employed technique. The limit of detection is the analyte level that with sufficiently high probability will lead to a correct positive detection. The obtained figures of merit (Table 5) can be employed for method comparison, and for assessing the detection capabilities of the proposed methodology.

Table 5. Results obtained by applying PARAFAC to the test binary mixtures

Sample	OXA (mg L^{-1})		PHE (mg L^{-1})	
	Nominal	**Predicted**	**Nominal**	**Predicted**
A	0.427	0.434	0.178	0.28
B	0.453	0.457	0.556	0.65
C	0.064	0.096	1.594	1.52
D	0.456	0.457	1.916	1.93
E	0.316	0.341	1.930	1.90
F	0.250	0.261	1.000	1.04
RMSEP (mg L^{-1})	0.017		0.068	
REP(%)	4.91		4.93	
Sensitivity (FU L mg^{-1})	1900		300	
Selectivity	0.12		0.12	
Analytical sensitivity (L mg^{-1})	920		140	
Detection limit (mg L^{-1})	0.004		0.02	

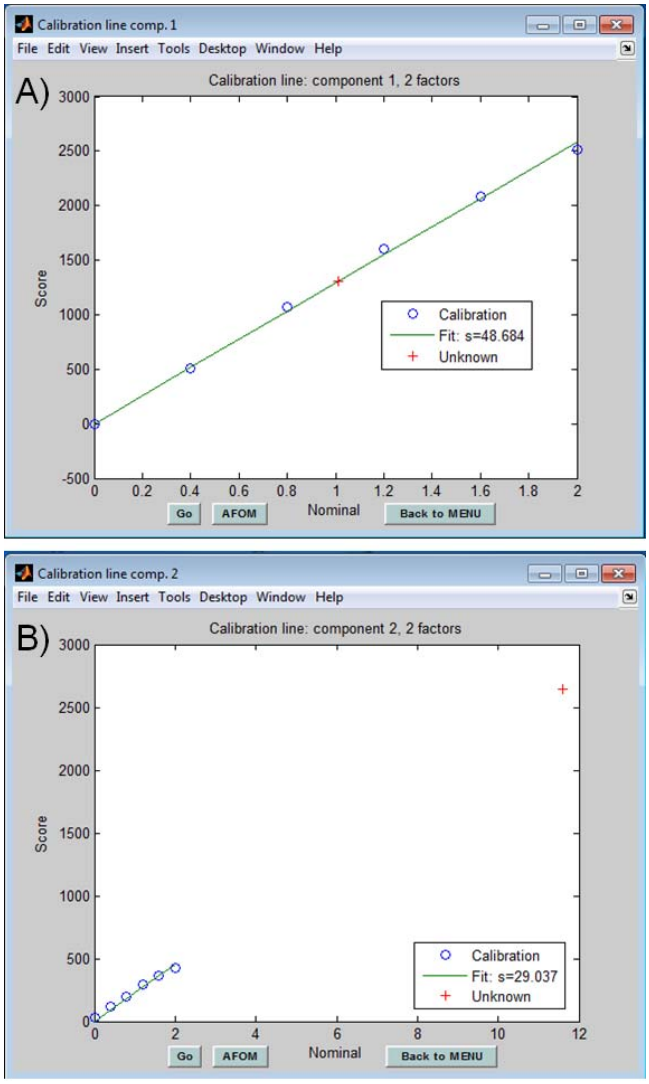

Figure 7. Pseudo-univariate calibration line obtained from PARAFAC decomposition of the three-way array built with the calibration samples and the target test sample, as calculated by mvc2basic. In the "PARAFAC profiles" window, the analyte is: A) correctly identified or B) misidentified.

Conclusion

The proposed experiment properly combines key concepts related to fluorescence and multivariate calibration methods through a practical analytical application. Discussions with the students during this work allows for an understanding of some aspects of advanced chemometrics, especially those related to the determination of one or more analytes in the presence of interferent species with overlapped signals. This contact with chemometrics opens up the possibility of applying other methods for the resolution of different situations. The students learn that one of the major advantages of the multivariate analysis of complex data sets built with multiple variables measured for many samples is the possibility of decomposing signals which would otherwise be difficult to separate, either visually or with classical mathematical approaches.

The approach of combining excitation-emission matrix fluorescence spectroscopy as analytical technique on one hand, and PARAFAC data processing on the other, was applied here to quantitatively determine two pharmaceutical drugs from heavily overlapped spectral data. This is a non-destructive procedure which does not require expensive reagents and laborious sample preparation prior to analysis. The experiments are simple and the results are obtained by easy measurements of fluorescence data and straightforward analysis through the mvc2basic graphical interface. Students can be encouraged to perform a literature search and to write a laboratory report to complete the learning process.

Acknowledgment. Financial support provided by the University of Rosario, CONICET and ANPCyT (Project No. PIP 2010-0084) is appreciated. Janssen-Cilag Laboratories and POEN SACIFI Laboratories (Buenos Aires, Argentina) are acknowledged for the supply of the pharmaceutical drugs. Valeria Boeris is grateful to CONICET for her scholarship.

Supporting Materials. A zip file containing mvc2basic_manual, mvc2basic_program, and mvc2basic_simulated_example files are available (http://dx.doi.org/10.1333/s00897132491a).

References and Notes

1. Richter, M. M. *Chem. Educator* **2001**, *6*(*1*), 21; DOI 10.1007/s00897000453a.
2. Bigger, S. W.; Ghiggino, K. P.; Meilak, G. A.; Verity, B. *J. Chem. Educ.* **1992**, *69*(*2*), 675; DOI 10.1021/ed069p675.
3. Barghouthi, S. A.; Perrault, J.; Holmes, L. H. *Chem. Educator* **1998**, *3*(*5*), 1 DOI 10.1007/s00897980254a.

4. Kubo, H.; Kobayashi, Y.; Kinoshita, T. *Anal. Chem.* **1986**, *58*(*13*), 2653; DOI 10.1021/ac00126a017.
5. Kruatong, T.; Dahsah, C.; Panijpan, B. *Chem. Educator* **2010**, *15*(*5*); DOI 10.1007/s00897102228a.
6. Carrillo-Carrión, C.; Simonet, B. M.; Valcárcel, M. *Anal. Chim. Acta* **2011**, *692*(*1–2*), 103; DOI 10.1016/j.aca.2011.03.003.
7. Rodríguez, N.; Real, B. D.; Cruz Ortiz, M.; Sarabia, L. A.; Herrero, A. *Anal. Chim. Acta* **2009**, *632*(*1*), 42; DOI 10.1016/j.aca.2008.10.051.
8. Escandar, G. M.; Olivieri, A. C.; Faber, N. M.; Goicoechea, H. C.; Muñoz de la Peña, A.; Poppi, R. J. *TrAC, Trends Anal. Chem.* **2007**, *26*(*7*), 752; DOI 10.1016/j.trac.2007.04.006.
9. Handbook of Near-Infrared Analysis, 3rd. Edition, D. A. Burns, Editor, CRC Press, Boca Raton, FL, 2008.
10. Roggo, Y.; Chalus, P.; Maurer, L.; Lema-Martinez, C.; Edmond, A.; Jent, N. *J. Pharm. Biomed. Anal.* **2007**, *44*(*3*):683; DOI 10.1016/j.jpba.2007.03.023.
11. Sorol, N.; Arancibia, E.; Bortolato, S. A.; Olivieri, A. C. *Chemom. Intell. Lab. Syst.* **2010**; *102*(*2*),100; DOI 10.1016/j.chemolab.2010.04.009.
12. Cozzolino, D.; Smyth, H. E.; Gishen, M. *J. Agric. Food. Chem.* **2003**, *51*(*26*), 7703; DOI 10.1021/jf034959s.
13. Booksh, K. S.; Kowalski, B. R. *Anal. Chem*. **1994**, *66*(*15*), 782A; DOI 10.1021/ac00087a718.
14. Olivieri, A. C. *Anal. Meth.* **2012**, *4*, 1876; DOI 10.1039/C2AY25064K.
15. Andersen, C.M.; Bro, R. *J Chemom.* **2003**, *17*(*4*), 200; DOI 10.1002/cem.790.
16. Bortolato, S. A.; Arancibia, J. A.; Escandar, G. M. *Anal. Chem.* **2008**, *80*(*21*), 8276; DOI 10.1021/ac801458a.
17. Bro, R. *Chemom. Intell. Lab. Syst.* **1997**, *38*(*2*), 149; DOI 10.1016/S0169-7439(97)00032-4.
18. Orzel, J.; Daszykowski, M.; Grabowski, I.; Zaleszczyk, G.; Sznajder, M.; Walczak, B. *Talanta* **2012**, *101*, 78; DOI 10.1016/j.talanta.2012.08.031.
19. Qing, X. D.; Wu, H. L.; Nie, C. C.; Yan, X. F.; Li, Y. N.; Wang, J. Y.; Yu, R. Q. *Talanta* **2013**, *103*, 86; DOI 10.1016/j.talanta.2012.10.012.
20. Hurtado Sánchez, M. C.; Durán Merás, I.; Rodríguez Cáceres, M. I.; Jiménez Girón, A.; Olivieri, A. C. *Talanta* **2012**, *88*, 609; DOI 10.1016/j.talanta.2011.11.045.
21. Muñoz de la Peña, A.; Espinosa Mansilla, A.; González Gómez, D.; Olivieri, A. C.; Goicoechea, H. C. *Anal. Chem*. **2003**, *75*(*11*), 2640; DOI 10.1021/ac026360h.
22. Olivieri, A. C.; Faber, N. M.; Ferré, J.; Boqué, R.; Kalivas, J. H.; Mark, H. *Pure Appl. Chem.* **2006**, *78*(*3*), 633; DOI 10.1351/pac200678030633.
23. Olivieri, A. C.; Wu, H. L.; Yu, R. Q. *Chemom. Intell. Lab. Syst.* **2009**, *96*(*2*), 246; DOI 10.1016/j.chemolab.2009.02.005.
24. Balraj, C.; Ganesh, K.; Elango, K. P. *Spectrochim. Acta*, Part A **2011**, *79*(5), 1137; DOI 10.1016/j.saa.2011.04.033.
25. Davies, J. E. *Occup. Environ. Med.* **2007**, *64*(*8*), e2; DOI10.1136/oem.2007.033902.
26. Lakowicz, J. R. Principles of fluorescence spectroscopy. 3rd. Edition, Springer, Berlin, 2006.
27. Marwood, C. A.; Solomon, K. R.; Greenberg, B. M. *Environ. Toxicol. Chem.* **2001**, *20*(*4*), 890; DOI 10.1002/etc.5620200425.
28. Bro, R.; Kiers, H. A. L. *J. Chemom*. **2003**, *17*(*5*), 274; DOI 10.1002/cem.801.
29. Wiberg, K.; Sterner Molin, A.; Jacobsson, S. P. *Talanta* **2004**, *62*(*3*), 567; DOI 10.1016/j.talanta.2003.08.024.
30. MATLAB version 2011b, The Mathworks Inc., Natick, Massachussets, USA.
31. Nepote, A. J.; Olivieri, A. C. *Anal. Chim. Acta* **2001**, *439*(*1*), 87; DOI 10.1016/S0003-2670(01)01018-2.
32. Arancibia, J. A.; Nepote, A. J.; Escandar, G. M.; Olivieri, A. C. *Anal. Chim. Acta* **2000**, *419*(*2*), 159; DOI 10.1016/S0003-2670(00)00993-4.